ORIGINAL RESEARCH ARTICLE

Preparations of Mo_2C or Mixture of Mo_2C and Mo by Silicon/Carbon Synergistic Reduction of Molybdenum Concentrate

HE-QIANG CHANG and GUO-HUA ZHANG

Molybdenum is one of the most widely used refractory metals, and about 80 pct of molybdenum is used in the iron and steel industries in the form of molybdenum additives. This work proposed a novel green strategy to prepare molybdenum additives with low S and Si contents through Si/C synergistic reduction of molybdenum concentrate, with the assistance of desulfurizer composed of CaO and C. The reaction mechanism as well as the effects of C and Si additions on reduction of molybdenum concentrate (which is one of the most important minerals for Mo extraction) with the main component of MoS_2 was studied in detail. After the sample was reacted at 1600 °C for 4 hours, a core–shell-structured product with molybdenum additive wrapped by the desulfurizer layer was obtained. For the raw material with a MoS_2:C:Si molar ratio of 6:6:4 reacted at 1600 °C for 4 h, Mo_2C with S and Si contents of 0.04 and 0.35 wt pct can be prepared. When the MoS_2:C:Si molar ratio was changed to 6:4:3.2, a mixture of Mo and Mo_2C can be prepared with C, S, and Si contents of 2.19, 0.13, and 0.23 wt pct, respectively. This work provides a sulfur-free emission method for the industrial production of carbon-containing molybdenum additives directly from molybdenum concentrate.

https://doi.org/10.1007/s11663-023-02767-8

I. INTRODUCTION

MOLYBDENUM is one of the most widely used refractory metals.[1,2] Because of its attractive physical and chemical properties such as high melting point, high elastic modulus, great high-temperature strength, superior thermal conductivity, excellent resistance to corrosion, and low coefficient of expansion, molybdenum and its compounds are extensively utilized in iron and steel, nuclear energy, catalysis, anti-corrosion, wear resistant, agriculture, and other fields.[3–8] In particular, the application of molybdenum in the iron and steel industries accounts for the vast majority, about 80 pct,[9] since the addition of molybdenum to iron and steel can improve their hardness, strength, toughness, creep resistance, thermal resistance, and corrosion resistance.[10,11] Molybdenum is added to iron and steel in the forms of molybdenum additives, including compacted molybdenum powder, molybdenum bar, ferromolybdenum, molybdenum trioxide block, calcium molybdate, carbon-reduced molybdenum, *etc.*[12] The mature production processes of these molybdenum additives are shown in Figure 1. Among these molybdenum additives, compacted molybdenum powder and molybdenum bar have the highest purity and are suitable for steels with strict requirements on molybdenum content and introduced impurities. However, the preparation of molybdenum powder and molybdenum bar requires a long process (Figure 1), resulting in the highest cost. Ferromolybdenum is the most commonly used molybdenum additive for alloying most steels and cast irons. However, the chemical composition of individual ferromolybdenum pieces in a single batch may vary widely due to the liquation processes in the melt.[12] Molybdenum trioxide block has the lowest price but contains harmful impurities. The addition of molybdenum trioxide will affect the production rhythm of steelmaking process, and part of MoO_3 will volatilization to lead to a low recovery rate. In order to avoid the volatilization of MoO_3, calcium molybdate prepared by roasting a mixture of roasted molybdenite and lime was proposed as a molybdenum additive. In addition,

HE-QIANG CHANG and GUO-HUA ZHANG are with the State Key Laboratory of Advanced Metallurgy, University of Science and Technology Beijing, Beijing, 100083, P.R. China and also with the Beijing Key Laboratory of Green Recovery and Extraction of Rare and Precious Metals, University of Science and Technology Beijing, Beijing 100083, P.R. China. Contact e-mail: ghzhang0914@ustb.edu.cn

Manuscript submitted September 11, 2022; accepted February 26, 2023.

Article published online March 20, 2023.

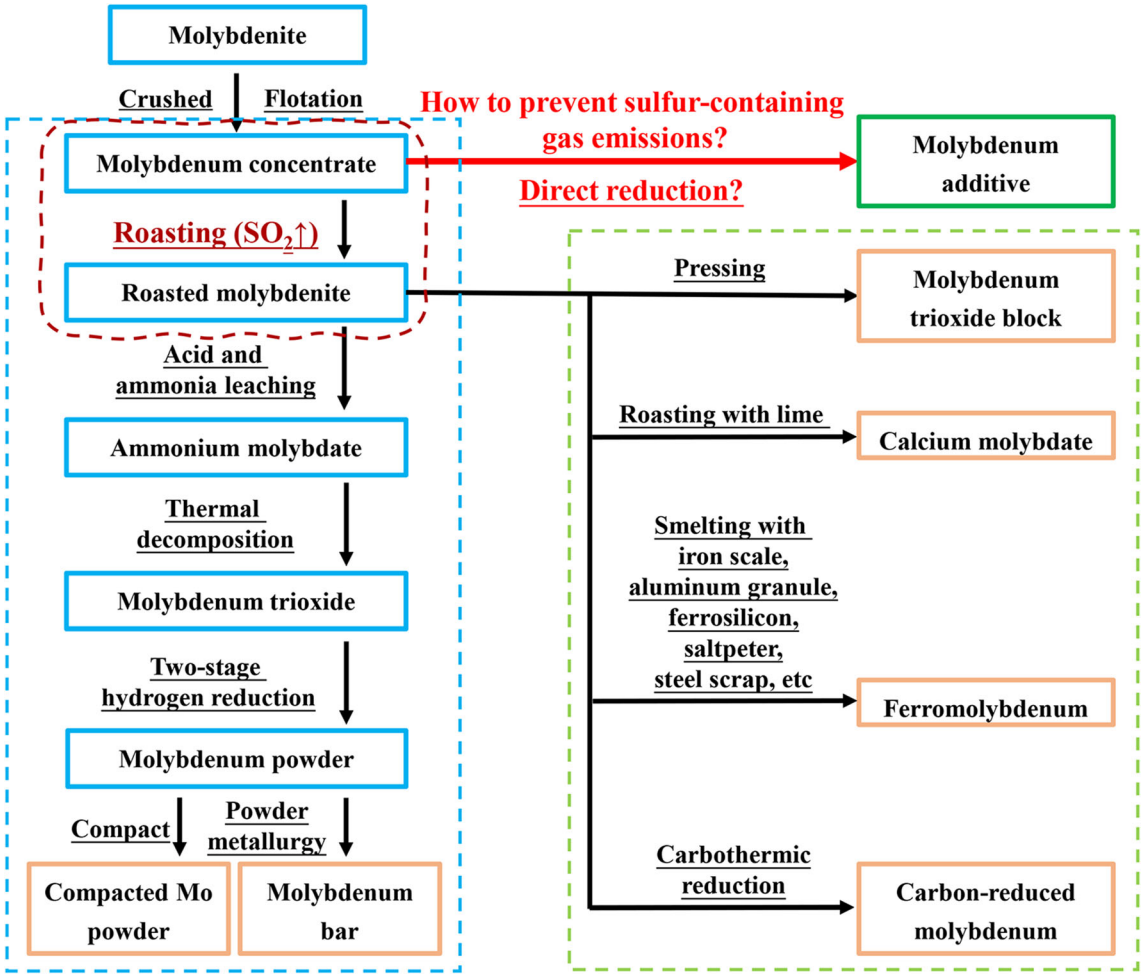

Fig. 1—Production process flow chart of main molybdenum additives.

carbon-reduced molybdenum is also an important molybdenum additive, which can be produced by carbothermal reduction of roasted molybdenite. However, in order to completely remove the oxygen, the residual carbon content is relatively large. This additive can be utilized for alloying cast iron (with the C and Si contents between 1.6 to 4.0 and 0.6 to 2.6 wt pct, respectively) and low alloy steels.

In China, molybdenite is the most important mineral for extracting molybdenum, and molybdenum concentrates with MoS_2 content of 85 to 96 pct can be obtained after crushing and flotation of molybdenite. As can be seen from Figure 1, for the pyrometallurgical process currently used in industrial production to extract Mo from molybdenum concentrate, the roasting of molybdenum concentrate (reaction [1]) to produce MoO_3 and SO_2 is an inevitable step. In general, economical way for the recovery of SO_2 in the form of H_2SO_4 requires a SO_2 concentration of higher than 3 pct. However, in order to ensure that Mo in MoS_2 is converted into MoO_3 as much as possible between 500 °C and 700 °C,[13–15] it is necessary to continuously introduce a large amount of air to guarantee sufficient oxygen supply, resulting in a low SO_2 concentration (not higher than 2 pct, and the reason will be explained in chapter 3.1 of this manuscript) in the generated flue gas.[16] In recent years, a variety of methods have been developed for harmless treatment of low-concentration SO_2 gas produced by oxidation roasting of molybdenum concentrate, including ammonia absorption method, wet lime and limestone scrubbing method, citrate method, active carbon absorption method, *etc*.[17–21] The ammonia absorption method used liquid ammonia or ammonium bicarbonate (NH_4HCO_3) as the adsorbent to absorb SO_2 to generate ammonium sulfite ($(NH_4)_2SO_3$), and the tail gas produced can meet the emission standard.[17] The wet lime and limestone scrubbing method used lime and limestone as the adsorbent to react with SO_2 to produce calcium sulfite ($CaSO_3$), and then oxidizes to form calcium sulfate ($CaSO_4$).[18,19] During the citrate method, SO_2 in flue gas was absorbed by aqueous sodium citrate solution, and dissolved SO_2 was subsequently recovered from the solution by steam stripping or other regenerative method, or the resulting absorbent

solution reacted with H_2S to obtain sulfur, which can be separated by flotation.[20] In addition, activated carbon adsorption method utilized the porosity of activated carbon to absorb SO_2 in flue gas.[21] Besides the above methods, Jinduicheng Molybdenum Industry Co., Ltd. mixed the flue gases produced by roasting pyrite and molybdenum concentrate, respectively. The total concentration of SO_2 in the obtained mixed flue gas was about 6 pct, which met the requirements for the preparation of sulfuric acid.[22] Nevertheless, the harmless treatment of low-concentration SO_2 gas will increase the production cost of molybdenum products. Therefore, it is particularly urgent to develop a green molybdenum extraction route without sulfur-containing gas emission:

$$MoS_2(s) + 3.5O_2(g) = MoO_3(s) + 2SO_2(g). \quad [1]$$

Over the past few decades, in order to reduce environment pollution caused by sulfur-containing gas emissions in the molybdenum extraction industry, many routes have been proposed,[10,23–37] such as vacuum thermal decomposition of molybdenum concentrate (reaction [2]),[25,26] roasting of molybdenum concentrate in the presence of soda or lime (reactions [3] and [4]),[27] direct reduction of molybdenum concentrate in the presence of desulfurizer (lime-assistant hydrothermal reduction, lime, or soda-assistant carbothermal reduction) (reaction [5]),[28–32] and direct electrolytic reduction of molybdenum sulfide.[37] Vacuum thermal decomposition of MoS_2 seems to be the optimal molybdenum extraction route among the above strategies, as the temperature required for decomposition of MoS_2 to yield Mo and S_2 can be lowered by reducing the vacuum degree.[26,33] Nevertheless, condensation of sulfur vapor in the low-temperature area will cause blockage of pipelines of vacuum equipment and cause accidents. Thus, there are still some problems to be overcome in the direct decomposition of molybdenum concentrate to prepare Mo powder. In addition, lime- or soda-assisted roasting of molybdenum concentrate makes the Mo and S elements in MoS_2 transform to $CaMoO_4$ or Na_2MoO_4, as well as $CaSO_4$ or Na_2SO_4. Subsequently, Mo element in $CaMoO_4$ can be selectively separated into H_2MoO_4 by hot sulfuric acid leaching, while Mo element in Na_2MoO_4 can be extracted in the form of MoO_3 by hot water leaching followed by NH_4Cl solution leaching and calcination steps.[27,34,35] Besides the above two strategies, direct reduction of molybdenum concentrate in the presence of desulfurizer may be an efficient molybdenum extraction strategy. The introduction of CaO or Na_2CO_3 can significantly reduce the reaction temperature between reducing agents (C, CO, CH_4, or H_2) and MoS_2, because CaO or Na_2CO_3 will preferentially react with MoS_2 to form molybdates $CaMoO_4$ or Na_2MoO_4 (reactions [6] and (7)).[28,29,32,36] However, in this route, acid leaching or water leaching treatment is required to remove the desulfurization product CaS or Na_2S, which releases harmful H_2S gas.

$$MoS_2(s) = Mo(s) + S_2(g), \quad [2]$$

$$MoS_2(s) + 3Ca(OH)_2(s) + 4.5O_2(g) = CaMoO_4(s) + 2CaSO_4(s) + 3H_2O(g), \quad [3]$$

$$MoS_2(s) + 3Na_2CO_3(s) + 4.5O_2(g) = Na_2MoO_4(s) + 2Na_2SO_4(s) + 3CO_2(g), \quad [4]$$

$$MoS_2(s) + (CaO, Na_2CO_3)(s) + (C, CO, CH_4, H_2)(\text{s or g}) \rightarrow (Mo_2C, Mo)(s) + (CaS, Na_2S)(s) + (CO, CO_2, H_2O)(g), \quad [5]$$

$$3MoS_2(s) + 8CaO(s) = 2CaMoO_4(s) + Mo(s) + 4CaS(s), \quad [6]$$

$$MoS_2(s) + 3Na_2CO_3(s) = Na_2MoO_4(s) + 2Na_2S(s) + 2CO_2(g) + CO(g). \quad [7]$$

In view of the above facts, Zhang[5] proposed a sulfur-free emission strategy for molybdenum extraction via carbothermal reduction of MoS_2, that is, the mixture of MoS_2 and C wrapped by a desulfurizer composed of CaO and C reacted at high temperatures to generate Mo_2C or Mo. After the completion of the reaction, a specimen with a core–shell structure can be obtained, and the target molybdenum-containing product can be collected by breaking the desulfurization product shell. The CS_2 gas generated by carbothermal reduction MoS_2 can be captured as CaS by the wrapped desulfurizer. Besides C, Si is also an important reduction agent for the reduction of MoS_2. Our team studied the preparation of $MoSi_2$ by silicothermic reduction of MoS_2 and found that the starting temperature for silicothermic reduction of MoS_2 is about 900 °C,[38] which is much lower than the carbothermic reduction temperature of MoS_2 (about 1300 °C).[5] Therefore, the introduction of Si is beneficial for lowering the reaction temperature. However, the price of silicon is higher than that of carbon, so the carbon should be dominant in the reducing agent.

According to the previous study, the dominated sulfur-containing gaseous product should be CS_2 during carbothermal reduction of MoS_2, and the molar ratio of MoS_2:C should be 1:1.5 to prepare Mo_2C (reaction [8]).[5] In addition, it has been reported that the sulfur-containing gaseous product is SiS during the preparation of $MoSi_2$ by silicothermic reduction of MoS_2 at 1000 to 1200 °C,[38] that is, 2 mol of Si is

required to remove S from 1 mol MoS_2, and the molar ratio of MoS_2:Si should be 1:2 for the synthesis of Mo by silicothermic reduction of MoS_2 (reaction [9]). In view of the above results, assuming that MoS_2 in the molybdenum concentrate with a proportion of x is reduced by C to form Mo_2C and CS_2, and the remaining part of 1-x is reduced by Si to generate Mo and SiS. The overall reaction can be expressed as reaction [10].

$$MoS_2(s) + 1.5C(s) = 0.5Mo_2C(s) + CS_2(g), \quad [8]$$

$$MoS_2(s) + 2Si(s) = Mo(s) + 2SiS(g), \quad [9]$$

$$MoS_2(s) + 1.5xC(s) + 2(1 - x)Si(s) = 0.5xMo_2C(s) + xCS_2(g) + (1 - x)Mo(s) + 2(1 - x)SiS(g). \quad [10]$$

Hence, the aim of this work is to prepare molybdenum additives with low S and Si contents via silicon/carbon synergistic reduction of molybdenum concentrate, while achieving the goal of sulfur-free emission. In addition, the reaction mechanism as well as the effects of carbon and silicon additions on the Si/C synergistic reduction of molybdenum concentrate was studied in detail.

II. MATERIALS AND METHODS

A. *Raw Materials*

High-purity molybdenum concentrate (MoS_2, 95.96 pct purity, Jinduicheng Molybdenum Industry Co., Ltd.) was utilized as the molybdenum source, and its main elemental composition is shown in Table I. Carbon black powder (C, 99 pct purity, Mitsubishi Chemical Corporation) and silicon powder (Si, 99 pct purity, Sinopharm Chemical Reagent Co., Ltd) were used as reductant. The microscopic morphologies of the raw materials are shown in Figure 2. It can be found that the used molybdenum concentrate (MoS_2) shows a layered structure with a lateral size of tens of microns (Figure 2(a)); the Si particles with a diameter of several microns are composed of a large amount of ultrafine Si grains (Figure 2(b)); and the particle size of spherical carbon black is about 50 nm (Figure 2(c)). Additionally, a mixture of lime (CaO, 97 pct purity, Sinopharm Chemical Reagent Co., Ltd) and carbon black was used as a desulfurizer.

Table I. Main Elemental Composition of Molybdenum Concentrate

Element	Mo	Si	Cu	Ca	Fe
Content, wt pct	57.35	0.91	0.023	0.17	0.47

B. *The Synthesis of Molybdenum Additives*

Firstly, the initial powders with different molar ratios of molybdenum concentrate, carbon black and Si were mixed uniformly thoroughly in an agate mortar for about 30 min, with 5 wt pct stearic acid as a binder (according to reaction [10]. Subsequently, 100 g of the mixed raw materials was pressed into a cylinder (diameter 36 mm and height 45 mm) under a uniaxial pressure of 300 MPa. Then, the cylinder was placed in a graphite crucible and wrapped with 100 g desulfurizer (consisting of CaO and C in a molar ratio of 2:1, according to reactions [11] and [12]). After that, the samples were put into the constant temperature zone of a vertical high-temperature furnace (with a diameter of 60 mm) and reacted at various temperatures for 4 h under an Ar (with a purity and flow rate of 99.99 pct and 300 ml/min, respectively) atmosphere. Finally, the desulfurization products and internal products were separated for further characterization.

$$2CaO(s) + C(s) + CS_2(g) = 2CaS(s) + 2CO(g), \quad [11]$$

$$3CaO(s) + 2SiS(g) = 2CaS(s) + Si(s) + CaSiO_3(s). \quad [12]$$

C. *Physical Characterizations*

The phase compositions of the as-prepared desulfurization products and internal products were determined by X-ray diffraction (XRD) (SMARTLAB(9), Rigaku Corporation, Akishima City, Japan). The carbon and residual sulfur contents of the synthesized samples were assessed by infrared carbon and sulfur analyzer (EMIA-920V2, HORIBA, Kyoto, Japan). The Si content of the products was measured by inductively coupled plasma atomic emission spectrometer (ICP-AES) (Plasma 2000, NSC, Beijing, China). Additionally, thermodynamic calculations in this work were performed by FactSage 8.2.

III. THERMODYNAMIC CALCULATION

A. *The Equilibrium Relationship Between SO_2 and O_2 During the Roasting of Molybdenum Concentrate*

As far as we know, there is no article explaining why the SO_2 concentration is lower than 2 pct during the roasting of molybdenum concentrate. This will be explained from a thermodynamic point of view.

According to reaction [1], the number of moles of gas decreases during oxidative roasting. Therefore, according to the ideal gas state equation, the sum of the volume fractions of O_2 and SO_2 in the roasting process should be slightly less than the volume fraction of O_2 in the air (21 pct). Considering the continuous supply of air, the sum of the volume fractions of O_2 and SO_2 in the oxidation roasting system should be close to 21 pct. The

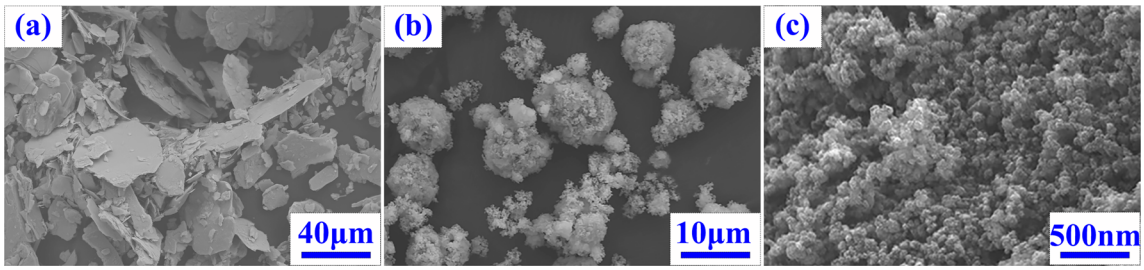

Fig. 2—The microscopic morphology of the raw materials of (*a*) molybdenum concentrate, (*b*) Si reagent, and (*c*) carbon black reagent.

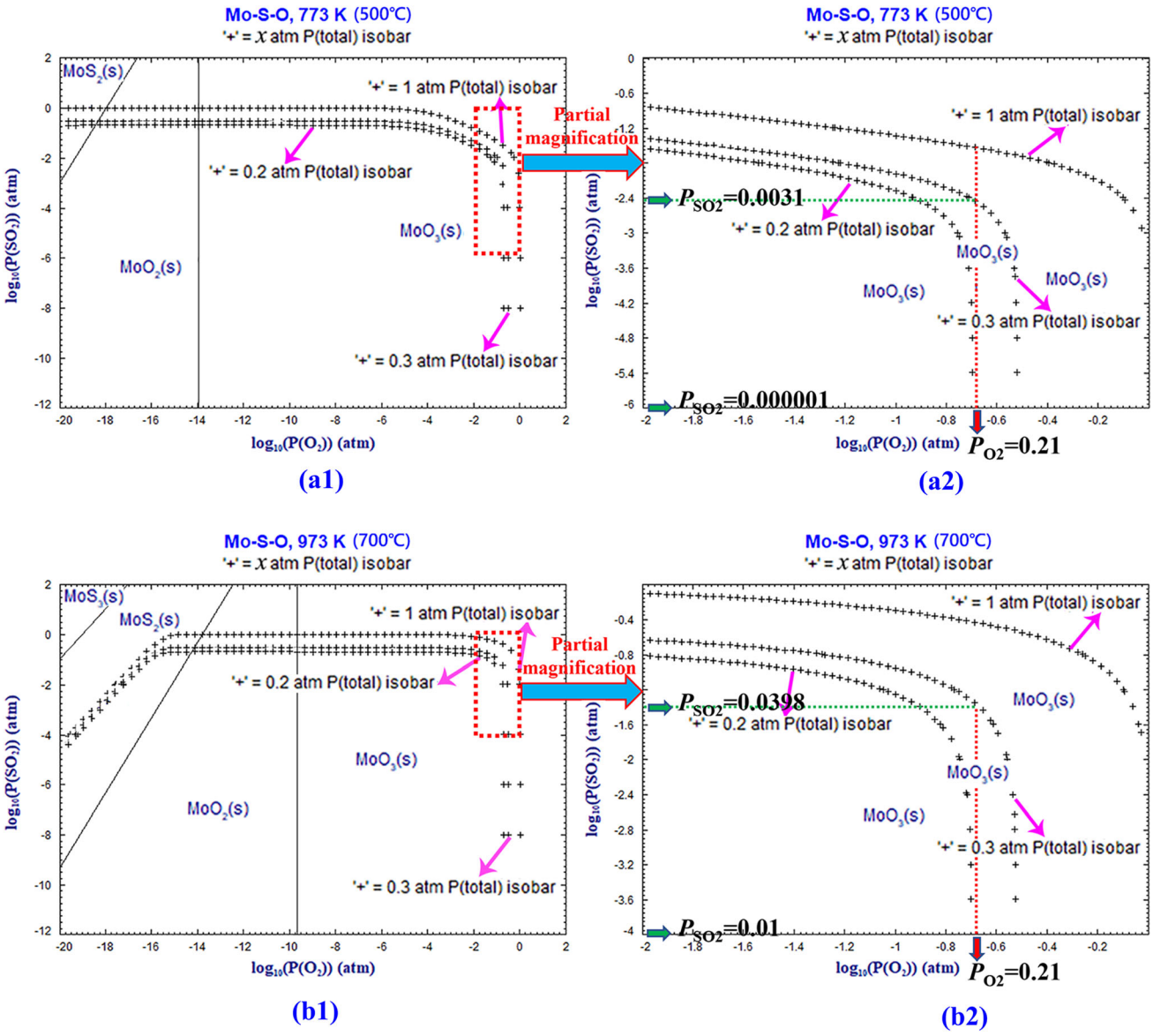

Fig. 3—Mo-S–O predominance area diagram plots at (a) 500 °C and (b) 700 °C.

Kellogg diagram of Mo-S–O system at 500 °C and 700 °C is shown in Figures 3(a) and (b), respectively. In Figures 3(a) and (b), there are three isobars of $Po_2 + Pso_2$, which are 1 atm, 0.3 atm, and 0.2 atm. When the temperature is 500 °C, the equilibrium Pso_2 in the system should be between 0.000001 (corresponding to $Po_2 + Pso_2 = 0.2$) and 0.0031 (corresponding to $Po_2 + Pso_2 = 0.3$), and thus, the SO_2 concentration should be between 0.0001 pct and 0.31 pct (Figures 3(a1) and (a2)). When the temperature rises to 700 °C, the

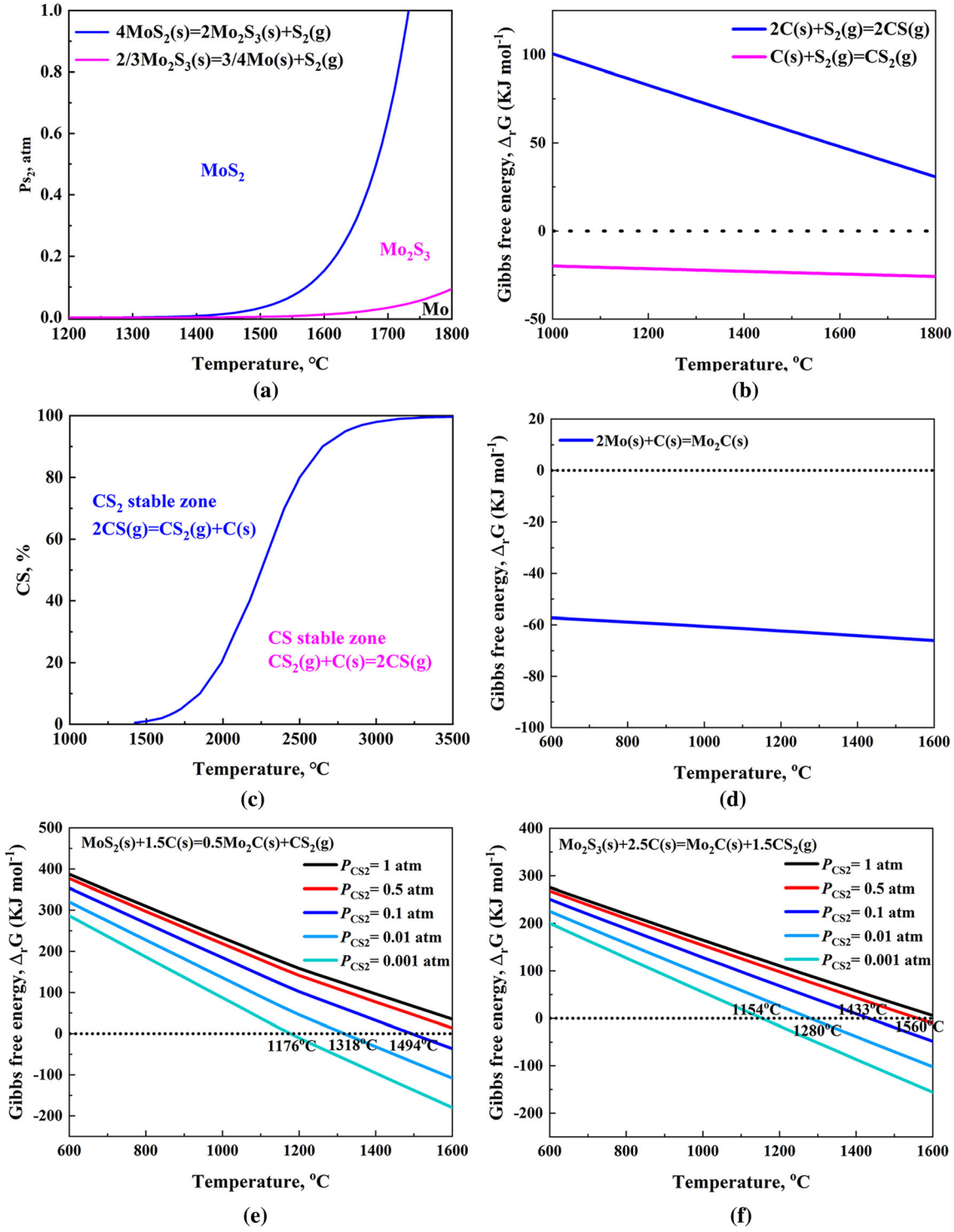

Fig. 4—(*a*) Equilibrium curves of the decomposition reaction of MoS_2 (reactions [13] and [14]); (*b*) temperature dependences of the standard Gibbs free energy changes of reactions [15] and [16]; (*c*) equilibrium curve of reaction [17]; (*d*) temperature dependences of the standard Gibbs free energy changes of reaction [18]; and temperature dependences of the standard reaction Gibbs free energy changes under various Pcs_2 of (*e*) reaction [8] and (*f*) reaction [19].

equilibrium Pso_2 in the system should be between 0.01 (corresponding to $Po_2 + Pso_2 = 0.2$) and 0.0398 (corresponding to $Po_2 + Pso_2 = 0.3$), and thus, the SO_2 concentration should be between 1 pct and 3.98 pct (Figures 3(b1) and (b2)). Due to the sum of the volume fractions of O_2 and SO_2 in the oxidation roasting system that should be close to 21 pct, the equilibrium Pso_2 in the system should be close to 1 pct. The above

thermodynamic results explain why the concentration of SO_2 produced during the oxidation roasting of molybdenum concentrate is not higher than 2 pct.

B. *Carbothermic reduction of MoS_2*

Many reports have demonstrated that the decomposition reaction of MoS_2 involves two steps.[33,39] MoS_2 is first decomposed into Mo_2S_3 and S_2 (reaction [13]). Then, Mo_2S_3 is further decomposed into Mo and S_2 (reaction [14]). The equilibrium curves of reactions [13] and [14] are plotted in Figure 4(a). Apparently, the decomposition reaction temperatures of MoS_2 and Mo_2S_3 are affected by the partial pressure of S_2 (Ps_2). Furthermore, under the same Ps_2, the decomposition of Mo_2S_3 requires a higher temperature than MoS_2. In addition, besides MoS_2 and Mo_2S_3, Mo-S compounds also contain MoS_3 and Mo_3S_4.[33,40,41]

$$MoS_2(s) = 0.5Mo_2S_3(s) + 0.25S_2(g), \quad [13]$$

$$0.5Mo_2S_3(s) = Mo(s) + 0.75S_2(g). \quad [14]$$

When C is added to Mo-S system, the formed S_2 may react with C according to reactions [15] and [16], and the corresponding changes of standard Gibbs free energy are shown in Figure 4(b). It can be clearly found that the standard Gibbs free energy of reaction [16] is negative in the temperature range of 1000 °C to 1800 °C, while it is positive for reaction [15], indicating that reaction [16] is thermodynamically feasible but reaction [15] is not in this temperature range under the standard condition. Therefore, it is difficult for S_2 to coexist with C from a thermodynamic point of view. Furthermore, CS_2 is prepared industrially using superheated sulfur vapor and charcoal at high temperature (700 °C to 900 °C) according to reaction [15]. Nevertheless, both CS_2 and CS may exist, as represented by reaction [17]. Assuming that there are only two gases, CS and CS_2, in the system, the equilibrium curve of reaction [17] is plotted in Figure 4(c). Obviously, temperature will affect the equilibrium Pcs and Pcs_2, and when the reaction temperature is lower than 1600 °C, the equilibrium Pcs is pretty low (less than 2 wt pct). Therefore, CS_2 will be the main gaseous product.

$$C(s) + S_2(g) = CS_2(g), \quad [15]$$

$$2C(s) + S_2(g) = 2CS(g), \quad [16]$$

$$C(s) + CS_2(g) = 2CS(g). \quad [17]$$

In addition to the reaction between C and S_2, C will also react with Mo, MoS_2, or Mo_2S_3. The Mo-C compounds contain three phases, Mo_2C, MoC, and $MoC_{(1-x)}$.[42,43] In view of the fact that only Mo_2C but no MoC and $MoC_{(1-x)}$ is generated in the carbothermal reduction of MoS_2,[5] only the related reactions involved Mo_2C are studied here. The change of standard Gibbs free energy of reaction [18] is shown in Figure 4(d), suggesting that Mo and C will react to form Mo_2C thermodynamically in the temperature range of 600 °C to 1600 °C. The changes of standard Gibbs free energy of reactions [8] and [19] under various Pcs_2 are shown in Figures 4(e) and (f) respectively, from which it can be clearly seen that the critical reaction temperatures are affected by the Pcs_2. In addition, for reactions [8] and [19], a lower Pcs_2 is beneficial to reduce the critical reaction temperature. The above thermodynamic results show that both low Ps_2 and Pcs_2 will promote the reaction of MoS_2.

$$Mo(s) + C(s) = Mo_2C(s), \quad [18]$$

$$Mo_2S_3(s) + 2.5C(s) = Mo_2C(s) + 1.5CS_2(g). \quad [19]$$

C. *Comparison of the Reducibility of Si and C*

The temperature dependences of the standard Gibbs free energy changes for the sulfurization reactions of C, Si, and Mo (reactions [15], [16,] and [20] through [23]) are plotted in Figure 5. Obviously, Si is easier to reduce MoS_2 or Mo_2S_3 to Mo than C, which is consistent with the experimental results in References 5 and 38 that the temperature required for the reduction of MoS_2 by Si is below C.

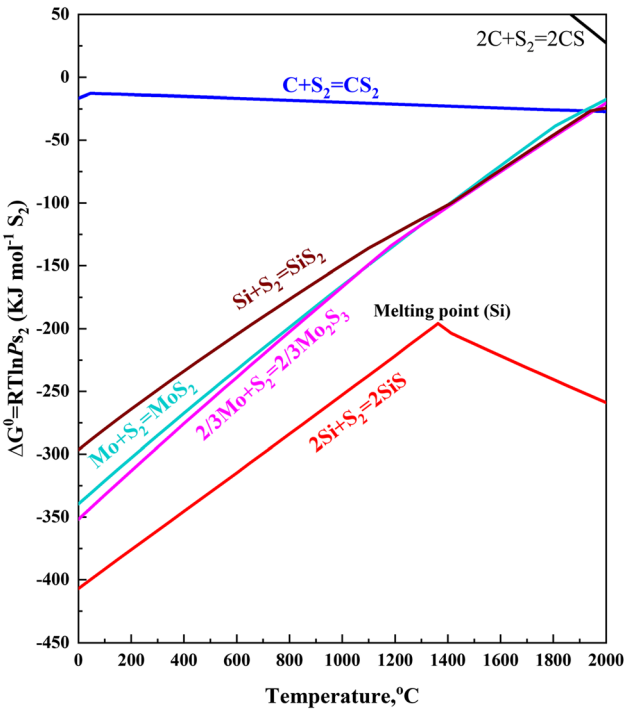

Fig. 5—Temperature dependences of the standard Gibbs free energy changes for the sulfurization reactions of C, Si, and Mo (reactions [15], [16] and [20] through [23]).

$$Si + S_2 = SiS_2, \quad [20]$$

$$2Si + S_2 = 2SiS, \quad [21]$$

$$Mo + S_2 = MoS_2, \quad [22]$$

$$2/3Mo + S_2 = 2/3Mo_2S_3. \quad [23]$$

IV. RESULTS AND DISCUSSION

The images of the raw materials and the typical product are shown in Figure 6. Clearly, after wrapping the sample with desulfurizer and reacting at 1600 °C for 4 h, a core–shell-structured target products can be obtained, and the target product (core) can be acquired after removing the desulfurization product (shell). In addition, the obtained Mo-containing product and desulfurized product were sintered under high-temperature conditions, resulting in sample shrinkage. After the reduction reaction, there is an obvious gap between desulfurization product and the core, which may be caused by the difference in mass change between core and desulfurization product layer before and after the reaction. For example, for 100 g of the mixed raw material with a MoS_2:C:Si molar ratio of 4:4:3.2, the mass of the core obtained after the reaction is only 53.06 g, while the mass of the shell increases from 100 to 128.88 g after the reaction. The differences in mass changes and the sintering of two parts at high reaction temperature make gap between core and shell.

A. *Phase Evolution Analysis*

First, the temperature dependence of the phase evolution of Si/C synergistic reduced product was investigated when the MoS_2:C:Si molar ratio was 6:6:4 (x in reaction [10] is equal to 4/6). Figure 7 plots the XRD patterns of samples prepared after reacting for 4 h at 800, 1000, 1200, 1400, 1500, and 1600 °C. Obviously, when the temperature is 800 °C, little to no reaction is observed since only the diffraction peaks of MoS_2 and Si can be identified. The absence of C diffraction peaks is due to the amorphous state of carbon black. When the temperature rises to 1000 °C, the diffraction peak intensity of MoS_2 decreases; the characteristic diffraction peaks of Si disappear, but the characteristic diffraction peaks of $MoSi_2$ appear. The reaction between MoS_2 and Si can be represented by reaction [24]. This result is consistent with the previous studies, that is, Si can completely react with MoS_2 at 1000 °C to form $MoSi_2$.[38] In addition, $MoSi_2$ disappears and Mo_2C appears when the temperature increases from 1000 °C to 1200 °C, and the overall reaction can be represented by reaction [25]. Figure 8 plots the equilibrium curve of reaction (25), where the abscissa and ordinate are temperature and partial pressure of SiS (P_{SiS}), respectively. Clearly, from a thermodynamic perspective, the reaction temperature of reaction [25] should be above 1280 °C when P_{SiS} is 1 atm. Nevertheless, due to the presence of the desulfurization layer, P_{SiS} should be far below 1 atm during the actual reaction, resulting in a lower critical reaction temperature. For example, the reaction temperature is 1200 °C when P_{SiS} is 0.326 atm. Furthermore, only Mo_2C can be identified in the products when the temperature is higher than 1400 °C, which indicates that almost all Mo in MoS_2 had reacted with C to produce Mo_2C.

$$MoS_2(s) + 4Si(s) = MoSi_2(s) + 2SiS(g), \quad [24]$$

$$MoS_2(s) + MoSi_2(s) + C(s) = Mo_2C(s) + 2SiS(g). \quad [25]$$

The C and residual S contents of the samples prepared after reacting at 1400, 1500, and 1600 °C for 4 h are shown in Figure 9, which are 5.46, 5.36, and 5.33 wt pct, as well as 2.48, 0.16, and 0.04 wt pct, respectively, and the corresponding contents of Mo_2C are calculated to be 92.82 wt pct, 91.12 wt pct, and 90.61 wt pct, respectively.

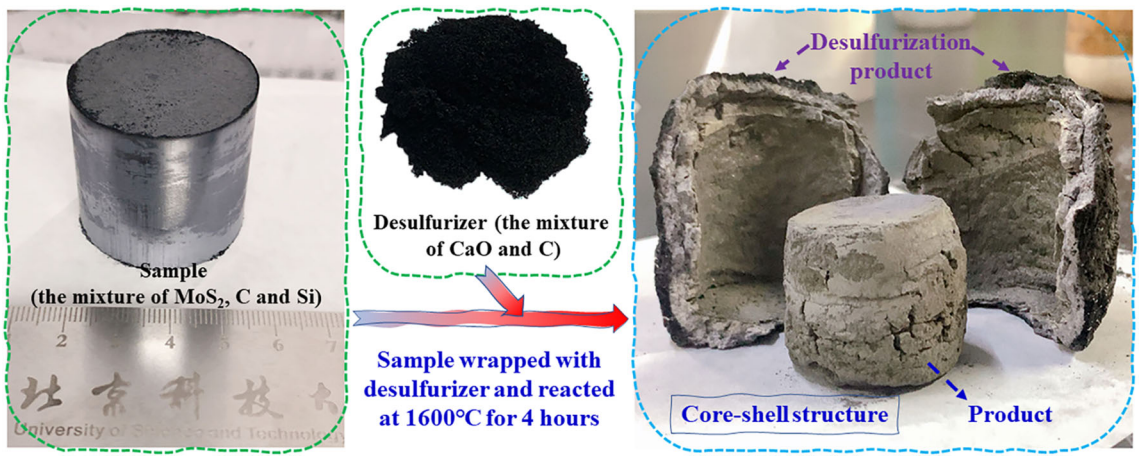

Fig. 6—Schematic diagram of the current process.

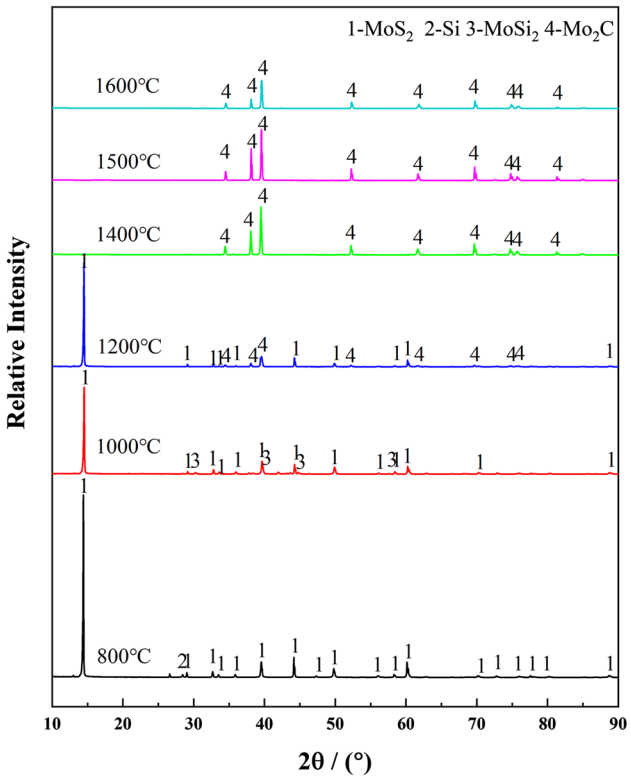

Fig. 7—XRD patterns of specimens obtained at 800 to 1600 °C with a MoS_2:C:Si molar ratio of 6:6:4.

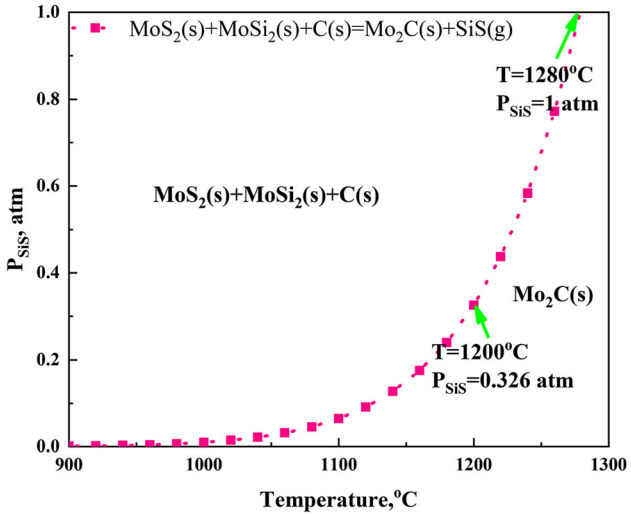

Fig. 8—Equilibrium curve of reaction [24].

Obviously, temperature is an important factor affecting the residual S content in the products. Additionally, the Si content of the sample prepared at 1600 °C was measured and is 0.35 pct. According to Chinese national standard (GB/T 3649-2008), the residual S content in commercial ferromolybdenum is generally not higher than 0.15 wt pct. In order to ensure that the residual S content in the product fulfill the standard, the experimental temperature is set to 1600 °C.

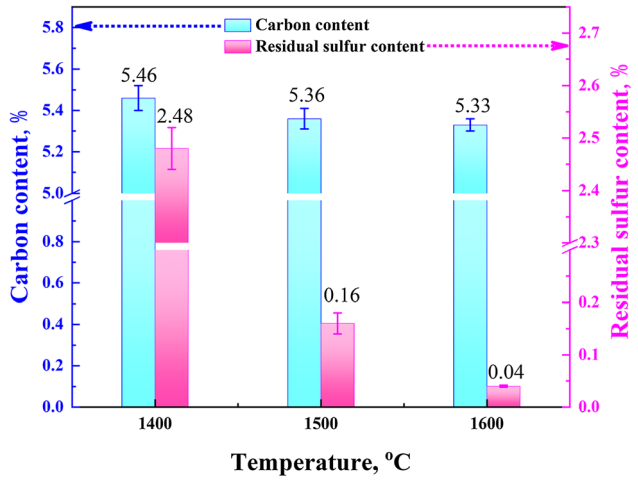

Fig. 9—Carbon and residual sulfur contents of samples prepared with a MoS_2:C:Si molar ratio of 6:6:4 at 1400, 1500, and 1600 °C.

From Figure 7, it can be found that only Mo_2C can be identified when the reaction temperature is above 1400 °C, which is inconsistent with the assumption in reaction [10]. This is probably due to the fact that the S-containing product produced by silicothermic reduction of MoS_2 under current conditions is a mixture of SiS and SiS_2 instead of just SiS. In order to further test whether this hypothesis (reaction [10]) is correct, five additional experiments (x in reaction [10] was set to 1/6, 3/6, 4/6, and 5/6, respectively) were performed at 1600 °C for 4 h, and the XRD patterns are shown in Figure 10. As can be seen from Figure 10, when x in reaction [10] is 1/6 and 2/6 (corresponding to MoS_2:C:Si, the molar ratios of 6:7.5:2 and 6:6:4, respectively), only Mo_2C can be obtained.

In our previous studies,[44] it was found that $MoSi_2$ can be prepared by silicothermic reduction of MoS_2 when the temperature was above 900 °C, and SiS_2 was preferentially formed under low temperature conditions. As the temperature rose, SiS_2 reacted with Si to form SiS. Furthermore, SiS gas can directly reduce MoS_2 to form $MoSi_2$ and SiS_2, and Mo_5Si_3 as well as Mo_3Si can be prepared after reacting at 1500 °C with the MoS_2:Si molar ratio of 1:1.7 and 1:2.33, respectively. Combining the results shown in Figure 7 and previous studies,[44] it can be concluded that reactions [24], [26], and [27] can occur during silicothermic reduction of MoS_2.[45] Figure 11(a) plots the equilibrium curves of reactions [24], [26], and [27] when the molar ratio of Si/MoS_2 is less than 3 (corresponding to reaction [28]. It can be seen that these three reactions are affected by the reaction temperature and P_{SiS}. In addition, Figure 11(a) can be divided into four thermodynamically stable regions, and the corresponding thermodynamically stable phase compositions from region I to region IV are MoS_2 + Si, $MoSi_2$ + SiS_2 + MoS_2, $MoSi_2$ + SiS_2 + SiS + MoS_2, and $MoSi_2$ + SiS + MoS_2, respectively. Moreover, from the viewpoint of thermodynamics, SiS_2 is more stable than SiS in region II (the overall reaction in region II can be expressed by reaction [28], while in region III, the thermodynamically stability of SiS_2 and

SiS is opposite to that in region II. For a sample with a Si/MoS_2 molar ratio of 4, when the temperature is above 1039 °C, the SiS_2 generated at low-temperature stage will react with Si to form SiS (the overall reaction can be represented by reaction [24]). However, the molar ratio of Si/MoS_2 under current condition is 2 (the part of MoS_2 that is assumed to react with C according to reaction [8] is not considered). This determines that the partially SiS_2 formed by silicothermic reduction of MoS_2 cannot converted into SiS with increasing temperature due to insufficient Si in the raw material. Therefore, the amount of MoS_2 reduced by C will be reduced, making the content of Mo_2C in the products prepared with a MoS_2:C:Si molar ratio of 6:7.5:2, 6:6:4 was higher than expected.

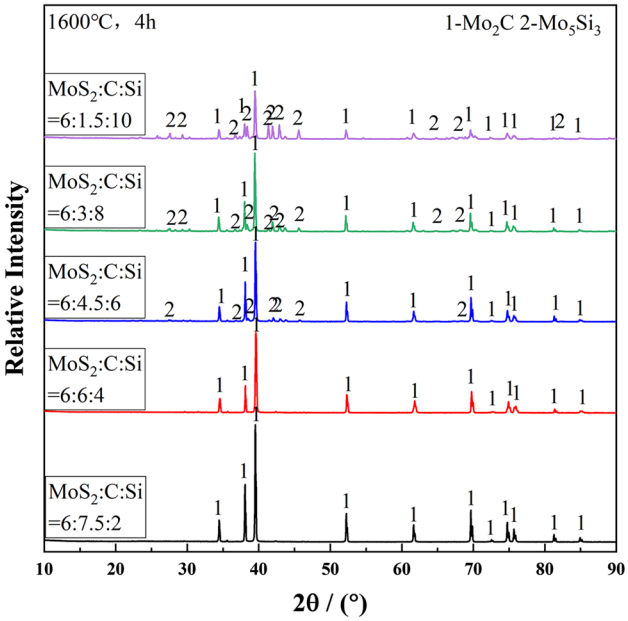

Fig. 10—XRD patterns of specimens obtained at 1600 °C with various MoS_2:C:Si molar ratio of 6:7.5:2, 6:6:4, 6:4.5:6, 6:3:8, and 6:1.5:10.

$$2SiS(g) \rightleftarrows SiS_2(s) + Si(s), \quad [26]$$

$$MoS_2(s) + 6SiS(g) = MoSi_2(s) + 4SiS_2(s), \quad [27]$$

$$MoS_2(s) + 3Si(s) = MoSi_2(s) + SiS_2(g). \quad [28]$$

As further increasing x to 3/6, 4/6, and 5/6, Mo_5Si_3 appears and gradually increases, while diffraction peak intensity of Mo_2C decreases. The formation of Mo_5Si_3 can be expressed by reaction [29]. As can be seen from Figure 7, $MoSi_2$ is preferentially formed during Si/C synergistic reduction of molybdenum concentrate at 1000 °C, and then $MoSi_2$ reacts with MoS_2 and C to produce Mo_2C. The S-containing product produced by silicothermic reduction of MoS_2 is a mixture of SiS and SiS_2 instead of just SiS, which leads to more $MoSi_2$ can be prepared than expected at 1000 °C (reaction [32]). According to reaction [10], as x decreases, the proportion of Si in the raw material increases, and thus, the amount of MoS_2 reduced by C decreases. Assuming that the ratio of SiS to SiS_2 in the product remains constant, when x decreases, the amount of $MoSi_2$ in the product will increase, and thereby, the molar ratio of the generated $MoSi_2$ to the MoS_2 reduced by C will increase. According to reaction [29], $MoSi_2$ can react with MoS_2 to form Mo_5Si_3. Figure 11(b) shows the equilibrium curves of reactions [29] through [31] when the molar ratio of Si/MoS_2 is less than 2 (corresponding to reaction [9]). Obviously, both reaction temperature and the molar ratio of Si/MoS_2 will affect the product phase composition. The thermodynamic results in Figure 11(b) also show that Mo_5Si_3 can be prepared by increasing the molar ratio of $MoSi_2$ to MoS_2.

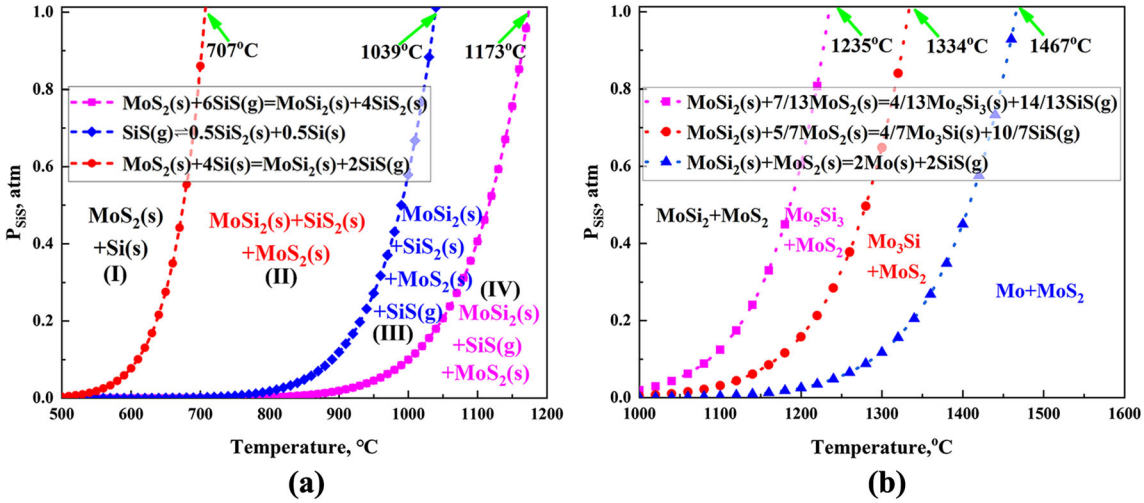

Fig. 11—Equilibrium curves of (a) reactions [24], [26], and [27] when the molar ratio of Si/MoS_2 is less than 3; (b) reactions [29] through [31] when the molar ratio of Si/MoS_2 is less than 2.

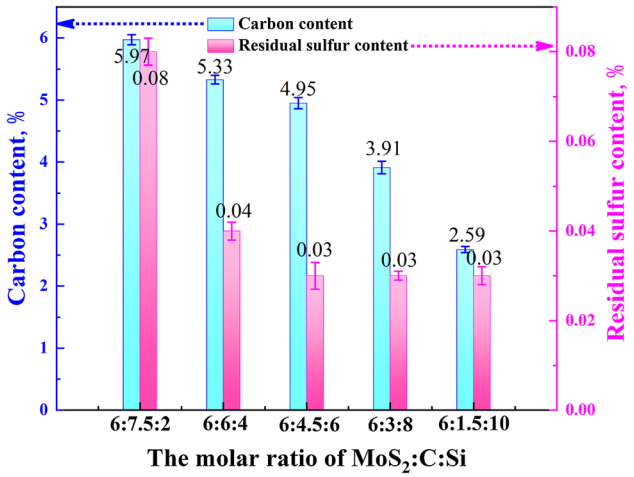

Fig. 12—Carbon and residual sulfur contents of the samples prepared with various MoS_2:C:Si molar ratios of 6:7.5:2, 6:6:4, 6:4.5:6, 6:3:8, and 6:1.5:10 at 1600 °C.

The C and residual S contents of those samples are shown in Figure 12. The C contents reduce with the decrease of C addition, and the residual S contents are all below 0.1 pct.

$$MoSi_2(s) + 7/13MoS_2(s) = 4/13Mo_5Si_3(s) + 14/13SiS(g), \quad [29]$$

$$MoSi_2(s) + 5/7MoS_2(s) = 4/7Mo_3Si(s) + 10/7SiS(g), \quad [30]$$

$$MoSi_2(s) + MoS_2(s) = 2Mo(s) + 2SiS(g), \quad [31]$$

$$MoS_2(s) + ySi(s) \rightarrow MoSi_2(s) + SiS(g) + SiS_2(g)\ (3 < y < 4). \quad [32]$$

V. EFFECTS OF C AND SI ADDITIONS ON SI/C SYNERGISTIC REDUCTION OF MOLYBDENUM CONCENTRATES

From Figure 10, it can be concluded that the Si/C synergistic reduction of MoS_2 is not as expected from reaction [10]. In order to select the appropriate raw materials ratio to synthesize the target product, it is necessary to investigate the influences of addition amounts of C and Si in the raw materials on the product. First, the effect of adding various amounts of C on the Si/C synergistic reduction of MoS_2 was explored with a fixed MoS_2:Si molar ratio of 6:4, and the molar ratios of MoS_2:C:Si were set to 6:5.4:4, 6:4.8:4, 6:4.2:4, 6:4:4, 6:3.6:4, 6:3.2:4, and 6:2.8:4, respectively.

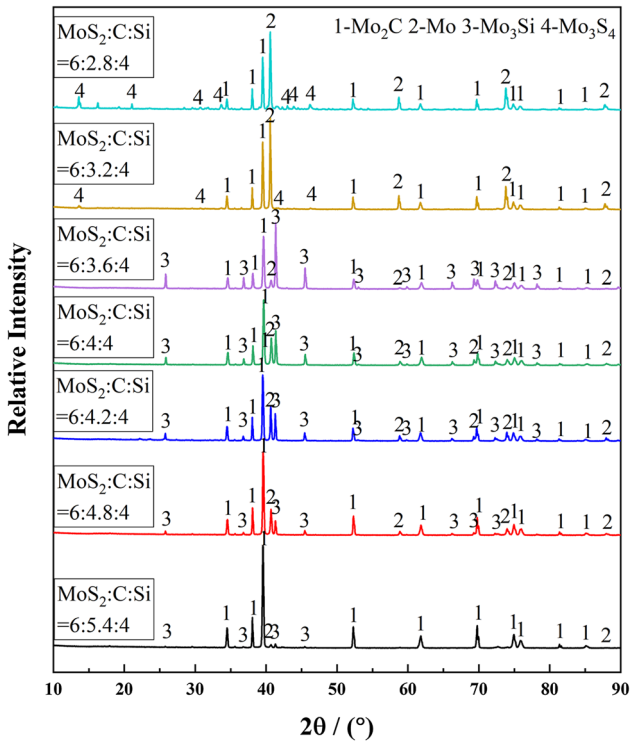

Fig. 13—XRD patterns of specimens obtained after reacting at 1600 °C for 4 h with various MoS_2:C:Si molar ratios of 6:5.4:4, 6:4.8:4, 6:4.2:4, 6:4:4, 6:3.6:4, 6:3.2:4, and 6:2.8:4.

Figure 13 shows the XRD patterns of the above seven samples after reacting at 1600 °C for 4 h. It can be found that the diffraction peak intensity of Mo_2C decreases with the reduce of C addition, and there are distinct diffraction peaks of MoS_2 when the molar ratios of MoS_2:C:Si is 6:3.2:4 and 6:2.8:4. When the molar ratio of MoS_2:C:Si is between 6:3.6:4 and 6:5.4:4, the diffraction peak intensity of Mo_3Si increases with the addition of C. In addition, it can be seen from Figure 13 that C exists only in the form of Mo_2C in the product. Assuming that all C only reacts with MoS_2 to form Mo_2C and CS_2 (reaction [8]), then the molar ratio of Si/MoS_2 (where the amount of MoS_2 is the total amount of MoS_2 minus the part of MoS_2 that reacts with C) decreases from 1.67 (corresponding to the MoS_2:C:Si molar ratio of 6:5.4:4) to 0.97 (corresponding to the MoS_2:C:Si molar ratio of 6:2.8:4) with decreasing carbon addition. As can be seen from Figure 11(b), when the molar ratio value of Si/MoS_2 is less 2, the reaction between $MoSi_2$ and MoS_2 is affected by the reaction temperature and P_{SiS}. In addition, the reaction between $MoSi_2$ and MoS_2 in the actual reaction process is also affected by the molar ratio of Si/MoS_2, and the phase transition with the decrease of Si/MoS_2 is $MoSi_2 \rightarrow Mo_5Si_3 \rightarrow Mo_3Si \rightarrow Mo$, which is basically consistent with the results shown in Figures 10 and 13.

The C and residual S contents of samples prepared with various C additions are plotted in Figure 14, and it is obvious that the C content reduces with the decrease of C addition. Additionally, C addition also affects the residual S content, which increases from 0.11 wt pct to 1.77 wt pct when the molar ratio of MoS_2:C:Si changes from 6:3.6:4 to 6:3.2:4.

Based on the MoS_2:C:Si molar ratio of 6:4:4, the effect of Si addition amount on the Si/C synergistic reduction of MoS_2 was studied by adjusting the addition amount of Si. Since the product prepared after reacting at 1600 °C for 4 h with a MoS_2:C:Si molar ratio of 6:4:4 contains Mo_3Si (Figure 13), it is necessary to reduce the amount of Si addition. Therefore, in this part of the experiments, the MoS_2:C:Si molar ratios were set to 6:4:3.6, 6:4:3.2, 6:4:2.8 and 6:4:2.4, respectively. The XRD patterns of samples prepared after reacting at 1600 °C for 4 h with various Si additions are shown in Figure 15. When the molar ratio of MoS_2:C:Si changes from 6:4:4 to 6:4:3.6 and then to 6:4:3.2, the diffraction peak intensity of Mo_3Si decreases and disappears, while that of Mo increases gradually. However, as further decreasing the amount of Si addition to 6:4:2.8 and 6:4:2.4, obvious MoS_2 diffraction peaks can be observed, suggesting that the amount of reducing agent is insufficient at this time.

The C and residual S contents of the samples prepared after reacting at 1600 °C for 4 h with various MoS_2:C:Si molar ratios of 6:4:3.6, 6:4:3.2, and 6:4:2.8 are plotted in Figure 16. For the product prepared with a MoS_2:C:Si molar ratio of 6:4:3.6, the C and residual S contents are 2.43 wt pct and 0.09 wt pct, respectively. In contrast, the C and residual S contents of the product prepared with a MoS_2:C:Si molar ratio of 6:4:3.2 are 2.19 wt pct and 0.13 wt pct, respectively. Furthermore, the Si contents of samples with MoS_2:C:Si molar ratios of 6:4:4, 6:4:3.6, and 6:4:3.2 are 2.04 wt pct, 0.67 wt pct, and 0.21 wt pct, respectively. Although the residual S content of the product prepared with a MoS_2:C:Si molar ratio of 6:4:3.2 is slightly higher than that of the product prepared with a MoS_2:C:Si molar ratio of 6:4:3.6, the C and Si contents are lower. Moreover, the former requires less Si addition than the latter. Therefore, considering the high price of Si and the residual S content in the product is already extremely low, the appropriate MoS_2:C:Si molar ratio for the preparation of molybdenum additive is 6:4:3.2.

From the above results, it can be seen that Mo_2C as well as mixture of Mo_2C and Mo with low S and Si contents can be prepared, which can be used as molybdenum additives for alloying cast iron low alloy steels.

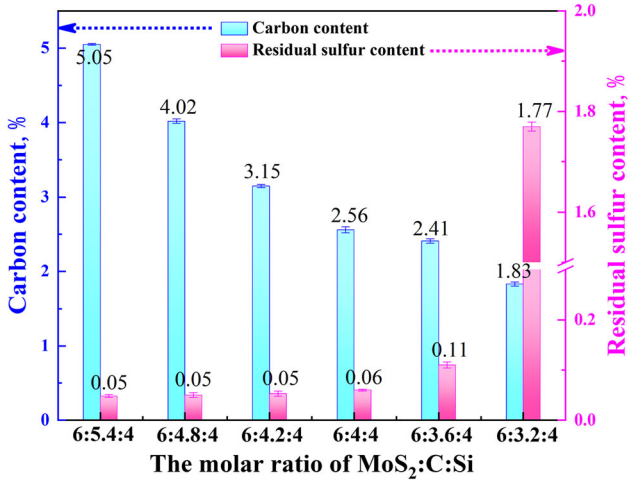

Fig. 14—Carbon and residual sulfur contents of the samples prepared at 1600 °C for 4 h with various MoS_2:C:Si molar ratios of 6:5.4:4, 6:4.8:4, 6:4.2:4, 6:4:4, 6:3.6:4, 6:3.2:4, and 6:2.8:4.

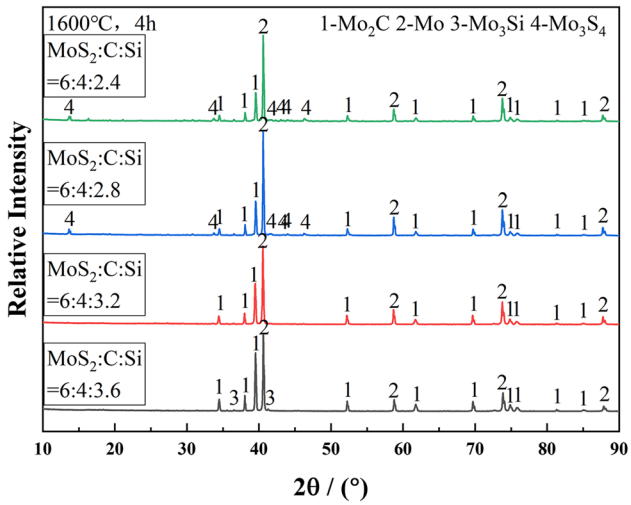

Fig. 15—XRD patterns of specimens obtained after reacting at 1600 °C for 4 h with various MoS_2:C:Si molar ratios of 6:4:3.6, 6:4:3.2, 6:4:2.8, and 6:4:2.4.

A. *Desulfurization Analysis*

As can be seen from Figure 6, after wrapping the sample with desulfurizer and reacting at 1600 °C for 4 h, a core–shell-structured product with molybdenum additive wrapped by the desulfurizer layer can be obtained.

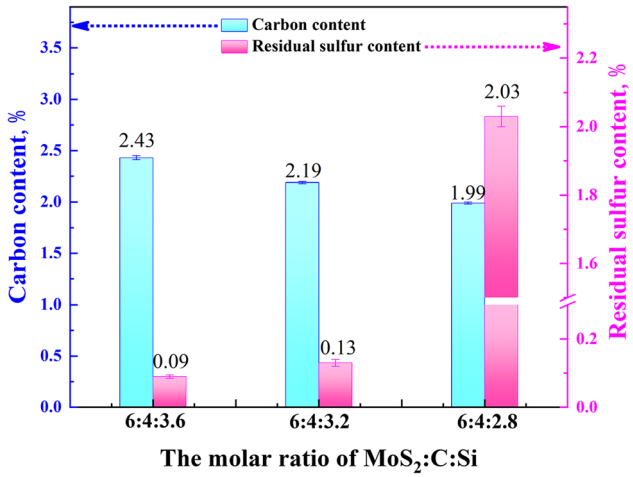

Fig. 16—Carbon and residual sulfur contents of the samples prepared at 1600 °C for 4 h with various MoS_2:C:Si molar ratios of 6:4:3.6, 6:4:3.2, 6:4:2.8, and 6:4:2.4.

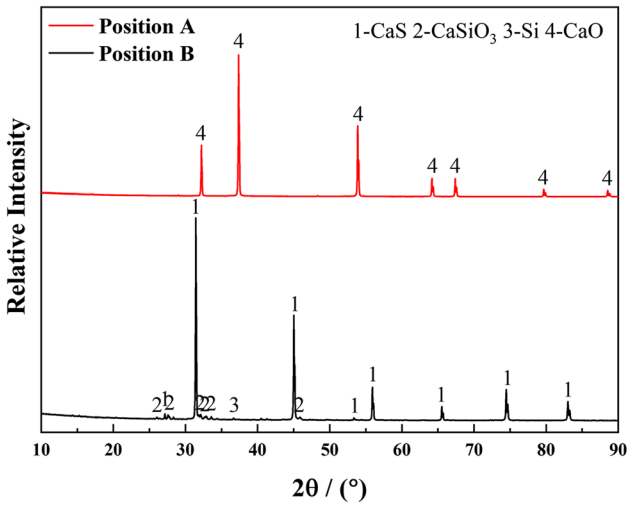

Fig. 17—XRD patterns of the desulfurization products corresponding to positions A and B in Figure 6.

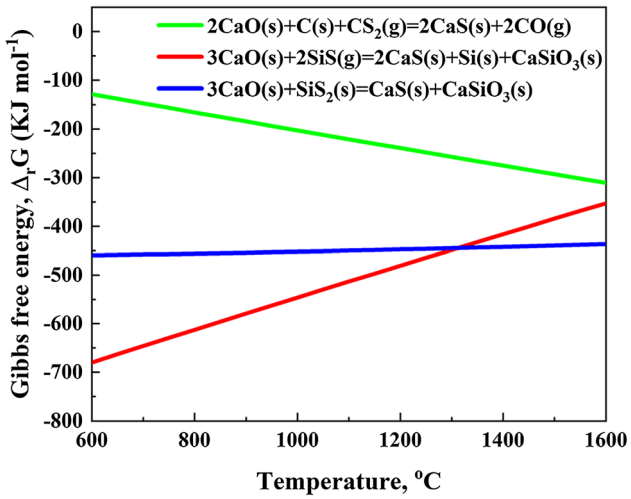

Fig. 18—Temperature dependences of the standard Gibbs free energy changes of desulfurization reactions of reactions [11], [12] and [33].

In order to determine the phase composition of the desulfurization product and whether all S in the raw material have been captured by desulfurizer, the desulfurization products corresponding to positions A and B in Figure 6 were collected for XRD testing, and the results are plotted in Figure 17. At position B, diffraction peaks of CaS, $CaSiO_3$, and Si can be identified, while the absence of CaO diffraction peaks suggests that all the CaO is involved in the desulfurization reaction. In addition, it can be concluded from the above analyses that CS_2, SiS, and SiS_2 will be generated during the Si/C synergistic reduction of molybdenum concentrate. Therefore, the desulfurization reaction may be expressed by reactions [11], [12], and [33]. At position A, only the diffraction peaks of CaO can be observed, revealing that all S in the forms of CS_2, SiS, and SiS_2 have been completely captured by the desulfurization layer close to the sample. In addition, the thermodynamic calculation results in Figure 18 also show that the desulfurization reactions (reactions [11], [12], and [33]) are thermodynamically feasible between 600 °C to 1600 °C. To sum up, in the current process, the mixture of CaO and C can be utilized as an effective desulfurizer.

$$3CaO(s) + SiS_2(s) = CaS(s) + CaSiO_3(s), \quad [33]$$

In our previous work,[45] the recovery of S in the desulfurization product was studied. In Reference 45, in order to separate sulfur-containing compounds from the desulfurization product (consisting of CaS, CaO, Ca_2SiO_4, and a small amount of Si) by an environmentally friendly way, a pyrometallurgical process for extracting and separating S was proposed, that is, the CaS in the desulfurization product was reacted with FeO to form FeS. In addition, the melting point of the reaction system was lowered by forming a low-basicity slag (mass ratio of CaO to SiO_2 was 0.6). After reacting at 1600 °C for 1 h in an Ar atmosphere, the sulfurization product and the low-basicity slag can be separated automatically due to density difference. The contents of FeS and Fe in the obtained sulfurization product were about 90 wt pct and 10 wt pct, respectively. Besides, S content of the obtained low-basicity slag was about 0.17 wt pct, revealing that most of the sulfur had been concentrated into the sulfurization product. The obtained sulfurization product FeS and Fe can be used as a vulcanizing agent for high-sulfur steel, and the low-basicity slag can be used for cement production. In this work, the desulfurization products consisted of CaS, $CaSiO_3$, CaO, and a small amount of Si, which were basically consistent with the composition of the desulfurization residue in Reference 45. Therefore, the harmlessness of desulfurization products and the resource utilization of S can also be realized with the same method.

S mass balance in the entire reaction system was evaluated. For the raw material with a MoS_2:C:Si molar ratio of 6:4:3.2, the mass of molybdenum concentrate in 100 g mixed raw material is 83.62 g, and the total mass of S is 32.09 g. After the reaction is completed, about 41.56 g unreacted desulfurizer (with the S content of about 0.001 wt pct) and 87.32 g desulfurization product (with the S content of 36.42 wt pct) can be obtained, and thus, the mass of S captured by desulfurizer is about 31.80 g. Additionally, the S content in the obtained Mo-containing product (53.06 g) is about 0.13 wt pct; thus, the mass of S in the acquired Mo-containing product is about 0.07 g. The total mass of S in desulfurization product and Mo-containing product is about 31.87 g, which is basically consistent with the total mass of S in raw materials. Consequently, no S in the sample is emitted into the environment.

VI. CONCLUSIONS

In this manuscript, a novel sulfur-free emission strategy to prepare molybdenum additives Mo_2C or mixture of Mo and Mo_2C by Si/C synergistic reduction of molybdenum concentrate was proposed. The reaction mechanism as well as the effects of C and Si addition on

the Si/C synergistic reduction of molybdenum concentrate was studied in detail. The following conclusions can be drawn:

1. The route of Si/C synergistic reduction of molybdenum concentrate can be used to produce molybdenum additives Mo_2C or mixture of Mo_2C and Mo with low S and Si contents. However, pure Mo was hard to be prepared.
2. With the increase of reaction temperature, when the molar ratio of Si/MoS_2 is less than 2, $MoSi_2$ is preferentially formed during Si/C synergistic reduction of molybdenum concentrate, and then $MoSi_2$ reacts with MoS_2 to produce Mo_5Si_3, Mo_3Si, or Mo. At the same time, C will participate in the reaction to generate Mo_2C or Mo. In addition, when the molar ratio of Si/MoS_2 is less 4, the S-containing product produced by silicothermic reduction of MoS_2 is a mixture of SiS and SiS_2 instead of just SiS.
3. The mixture of CaO and C can be used as an effective desulfurizer in this route and the sulfur-containing species CS_2, SiS, and SiS_2 produced by Si/C co-reduction of MoS_2 can be completely captured by the desulfurizer in the forms of CaS, $CaSiO_3$, and Si. In addition, S mass balance in the entire reaction system suggests that no S in the sample was emitted into the environment.
4. Mo_2C was acquired for the sample with a MoS_2:C:Si molar ratio of 6:6:4 after reacting at 1600 °C for 4 h, with C, S, and Si contents of 5.33 wt pct, 0.04 wt pct, and 0.35 wt pct, respectively. The mixture of Mo and Mo_2C can be prepared with a MoS_2:C:Si molar ratio of 6:4:3.2 after reacting at 1600 °C for 4 h, with C, S, and Si contents of 2.19 wt pct, 0.13 wt pct, and 0.23 wt pct, respectively.

ACKNOWLEDGMENTS

This work was financially supported by the State Key Laboratory of Advanced Metallurgy, University of Science and Technology Beijing, China.

CONFLICT OF INTEREST

There are no conflicts to declare.

REFERENCES

1. D.G. Barceloux and D. Barceloux: *J. Toxicol. Clin. Toxic.*, 1999, vol. 37, pp. 231–37.
2. C.K. Gupta: *Extractive Metallurgy of Molybdenum*, CRC Press, Boca Raton, 2017.
3. J.A. Novotny and C.A. Peterson: *Adv. Nutr.*, 2018, vol. 9, pp. 272–73.
4. L.L. Snead, D.T. Hoelzer, M. Rieth and A.A.N. Nemith: *Structural alloys for nuclear energy applications*, Elsevier, 2019, pp. 585–640.
5. H.Q. Chang, G.H. Zhang, and K.C. Chou: *Metall. Mater. Trans. B.*, 2022, vol. 53, pp. 96–106.
6. H.Q. Chang, G.H. Zhang, and K.C. Chou: *Electrochim. Acta.*, 2021, vol. 394, 139119.
7. D. Kosugi, T. Hagio, Y. Kamimoto, and R. Ichino: *Coatings*, 2017, vol. 7, p. 235.
8. B.N. Kaiser, K.L. Gridley, J. Ngaire Brady, T. Phillips and S.D. Tyerman: *Ann. Bot-london.*, 2005, vol. 96, pp. 745–54.
9. T. Outteridge, N. Kinsman, G. Ronchi, and H. Mohrbacher: *Adv. Manuf.*, 2020, vol. 8, pp. 35–39.
10. X.R. Chen, Q.J. Zhai, H. Dong, B.H. Dai, and H. Mohrbacher: *Adv. Manuf.*, 2020, vol. 8, pp. 3–14.
11. P.J. Cunat: *Euro Inox.*, 2004, vol. 2004, pp. 1–24.
12. M.S. Leitman, B.N. Nikonov, and V.V. Tregubenko: *Steel in Translation.*, 2007, vol. 37, pp. 1024–27.
13. T. Utigard: *Metall Mater Trans B.*, 2009, vol. 40B, pp. 490–96.
14. W. Lu, G. Zhang and Jie D: *T Nonferr Metal Soc.*, 2015, vol. 25), pp. 4167–74.
15. P.V. Aleksandrov, A.S. Medvedev, M.F. Milovanov, V.A. Imideev, S.A. Kotova, and D.O. Moskovskikh: *Int J Miner Process.*, 2017, vol. 161, pp. 13–20.
16. P.K. Tripathy, V.D. Shah, R.H. Rakhasia, J.C. Sehra: *Environmental and Waste Management.*, 1998, pp. 92–99.
17. Y.A. Zhu: *China Nonferrous Metallurgy.*, 2006, vol. 35, pp. 48–50. (**in Chinese**).
18. E. Bakke: *J Air Pollut Control.*, 1980, vol. 30, pp. 1157–61.
19. N. Rajendran, G. Latha, K. Ravichandran, and S. Rajeswari: *Corros Rev.*, 1999, vol. 17, pp. 443–66.
20. X. Jiang, L. Youzhi, and G.U. Meiduo: *Chin J Chem Eng.*, 2011, vol. 19, pp. 687–92.
21. R. Jamil, L. Ming, I. Jamil, and R. Jamil: *Int. J. Innov. Appl. Stud.*, 2013, vol. 4, pp. 286–97.
22. Y.L. Zheng and W.L Hou: *China Molybdenum Industry.*, 2005, vol. 29, pp. 32–34. (**in Chinese**).
23. P.M. Prasad, T.R. Mankhand, and A.J. Prasad: *NML Tech. J.*, 1997, vol. 39, pp. 39–58.
24. T.A. Lasheen, M.E. El-Ahmady, H.B. Hassib, and A.S. Helal: *Min. Proc. Ext. Met. Rev.*, 2015, vol. 36, pp. 145–73.
25. R.J. Munz and W.H. Gauvin: *AICHE J.*, 1975, vol. 21, pp. 1132–42.
26. L. Wang, P. Guo, J. Pang, and P. Zhao: *Vacuum*, 2015, vol. 116, pp. 77–81.
27. P.K. Tripathy and R.H. Rakhasia: *Min. Proc. Ext. Met.*, 2006, vol. 115, pp. 8–14.
28. F. Habashi and R. Dugdale: *Metall. Trans.*, 1973, vol. 4, pp. 1865–71.
29. T.R. Mankhand and P.M. Prasad: *Metall. Trans. B.*, 1982, vol. 13B, pp. 275–82.
30. R. Padilla, M.C. Ruiz, and H.Y. Sohn: *Metall. Mater. Trans. B.*, 1997, vol. 28B, pp. 265–74.
31. S. Ghasemi, M.H. Abbasi, A. Saidi, J.Y. Kim, and J.S. Lee: *Ind. Eng. Chem. Res.*, 2011, vol. 50, pp. 13340–46.
32. H.Q. Chang, K. He, G.H. Zhang, and K.C. Chou: *JOM.*, 2020, vol. 72, pp. 4030–41.
33. G.H. Zhang, H.Q. Chang, L. Wang, and K.C. Chou: *Int. J. Min. Met. Mater.*, 2018, vol. 25, pp. 405–12.
34. S. Singh, M.K. Chetty, J.M. Juneja, J.C. Sehra, and C.K. Gupta: *Miner. Eng.*, 1988, vol. 1, pp. 337–42.
35. J.M. Juneja, S. Singh, and D.K. Bose: *Hydrometallurgy*, 1996, vol. 41, pp. 201–09.
36. H.Q. Chang, G.H. Zhang, and K.C. Chou: *JOM.*, 2021, vol. 73, pp. 2540–48.
37. S.K. Sahu, B. Chmielowiec, and A. Allanore: *Electrochim Acta.*, 2017, vol. 243, pp. 382–89.
38. H.Q. Chang, G.H. Zhang, and K.C. Chou: *J. Am. Ceram. Soc.*, 2021, vol. 104, pp. 6092–99.
39. F. Liu, Y. Zhou, D. Liu, X. Chen, C. Yang, and L. Zhou: *Vacuum*, 2017, vol. 139, pp. 143–52.
40. L. Brewer and R.H. Lamoreaux: *Bulletin of alloy phase diagrams*, 1980, vol. 1, pp. 93–95.
41. P. Afanasiev: *C. R. Chim.*, 2008, vol. 11, pp. 159–82.
42. J.O. Andersson: *Calphad*, 1988, vol. 12, pp. 1–8.
43. K. Kuo and G. Hägg: *Nature*, 1952, vol. 170, pp. 245–46.
44. H.Q. Chang, H.Y. Wang, G.H. Zhang, and K.C. Chou: *Ceram. Int.*, 2022, vol. 48, pp. 7815–26.

45. R.O. Suzuki, Y. Yashima, T. Kaneko, E. Ahmadi, T. Kikuchi, T. Watanabe, and G. Nogami: *Metall Mater Trans B.*, 2021, vol. 52B, pp. 1379–91.